Supplementary Material for

Origin of Ligand-Driven Selectivity in Alkyne Semihydrogenation over Silica-Supported Copper Nanoparticles

Nicolas Kaeffer,[a,‡] *Kim Larmier,*[a,b,‡] *Alexey Fedorov,*[a,c] *Christophe Copéret*[a,]*

a) ETH Zürich, Department of Chemistry and Applied Biosciences, Vladimir-Prelog-Weg 1-5, CH-8093, Zürich, Switzerland.

b) Current address: IFP Energies nouvelles, Rond-Point de l'échangeur de Solaize, BP3, 69360 Solaize, France.

c) Current address: ETH Zürich, Department of Mechanical and Process Engineering, Leonhardstrasse 21, CH-8092 Zürich, Switzerland.

* ccoperet@inorg.chem.ethz.ch

Table of Contents

Gas adsorption isotherms

25

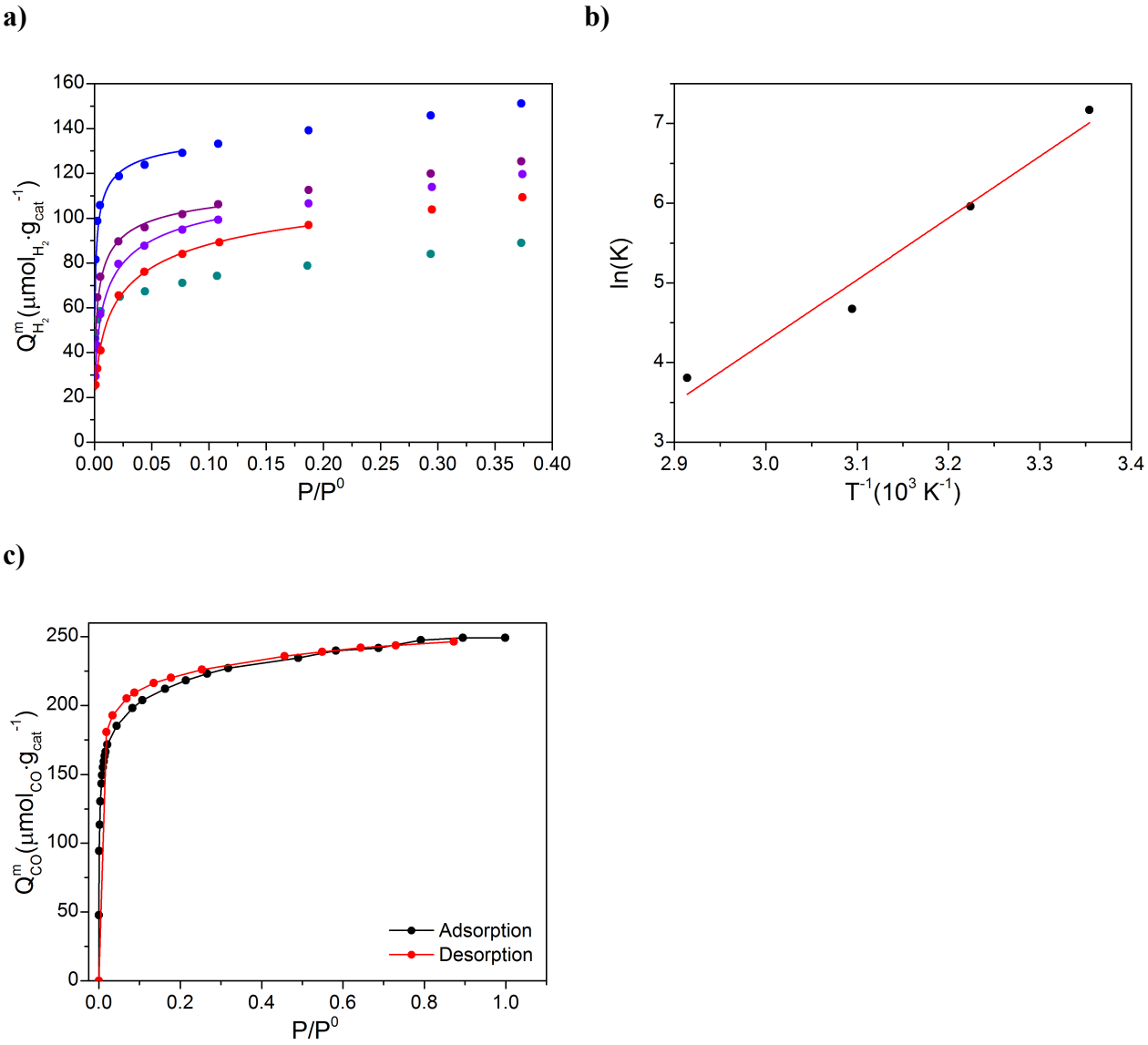

Figure S1. a) H_2 adsorption isotherms on **Cu/SiO$_2$** (dots) at 5 (cyan), 25 (blue), 37 (purple), 50 (violet) and 70 (red) °C with Langmuir dissociative adsorption isotherm fits (lines); b) ln(K_{H_2}) vs T^{-1} plot (dots) and associated linear fit (line); c) CO adsorption (black) and desorption (red) isotherms on **Cu/SiO$_2$** at 25 °C.

H_2 chemisorption curves were fitted with a Langmuir dissociative adsorption isotherm following:

$$Q_{H_2}(P) = Q_{H_2}^{max} \cdot \frac{\sqrt{K_{H_2}\frac{P}{P^0}}}{1+\sqrt{K_{H_2}\frac{P}{P^0}}} \qquad \textbf{Equation S1}$$

where Q_{H_2}, $Q_{H_2}^{max}$ are coverage and maximal coverage in H_2, respectively, while P and P^0 are partial and standard (1 bar) pressure in H_2 and K_{H_2} is the adsorption equilibrium constant for H_2.

Fitting H_2 isotherms allowed estimating the maximal surface coverage in H_2 as:

$$Q_{H_2}^{max} = 130\ \mu mol_{H_2} \cdot g_{cat}^{-1}$$

This figure is in agreement with the maximal coverage found by CO chemisorption (ca. $240\ \mu mol_{CO} \cdot g_{cat}^{-1}$), taking into account that H_2 occupies ca. two Cu sites,[1] whereas CO occupies one Cu site.

We estimated the standard adsorption enthalpy of H_2 on **Cu/SiO$_2$** using Van't Hoff equation:

$$\ln\left(K_{H_2}\right) = -\frac{\Delta H_{ads}^0}{R} \cdot T^{-1} + \frac{\Delta S_{ads}^0}{R} \qquad \textbf{Equation S2}$$

from which we could recover by the linear fitting of data presented in **Figure S1b**:

$$\Delta H_{ads}^0 = -64\ kJ \cdot mol^{-1}$$

Gas chromatography data

Table S1. Molar ratios (%) in hydrogenation products from GC analysis of final mixtures (16.3 h).

Ligand	**L/S**	**S**	(*Z*)-$\mathbf{S}_{2H}$	(*E*)-$\mathbf{S}_{2H}$	$\mathbf{S}_{4H}$
None	–	0	0	0	100
None	–	0	0	0	100
PCy_3	1:50	0	51	12	37
PCy_3	1:50	0	55	12	34
PCy_3	1:100	0	46	10	44
PCy_3	1:100	0	51	12	37
IMes	1:50	0	88	2	10

Determination of partial orders

The partial orders with respect to the concentration of alkyne [**S**], the concentration of catalyst [**cat**] and the pressure of hydrogen P_{H_2} have been determined for the first part of the curves, corresponding mainly to the hydrogenation of **S** to **S$_{2H}$**. We assumed that the rate expression is of the form

Equations S3

$$r = k[\mathbf{S}]^{\alpha}[\mathbf{cat}]^{\beta}\mathrm{P}_{H_2}^{\gamma}$$

We measured the rates under different sets of experimental conditions by systematic variations of only one of the [**S**], [**cat**] and P_{H_2} parameters. The two other parameters are set to the reference values used within the manuscript ([**S**] = 0.30 mol·L^{-1}, [**cat**] = 5.00 g_{cat}·L^{-1} and P_{H_2} = 10 bar). The obtained curves are linear in the first section, and the rates *r* are measured as the slope of these H_2 consumption curves. We then draw logarithmic plots of the experimental rates as a function of the varied parameter and obtain the respective partial order as the slope of the corresponding linear fit.

Partial order in [**S**]

Table S2. Experimental rates for determination of partial orders in [**S**]

Entry	[**S**] (mol·L^{-1})	*r* (mol·L^{-1}·h^{-1})
1	0.20	0.0306
2	0.15	0.0330
3	0.30	0.0315

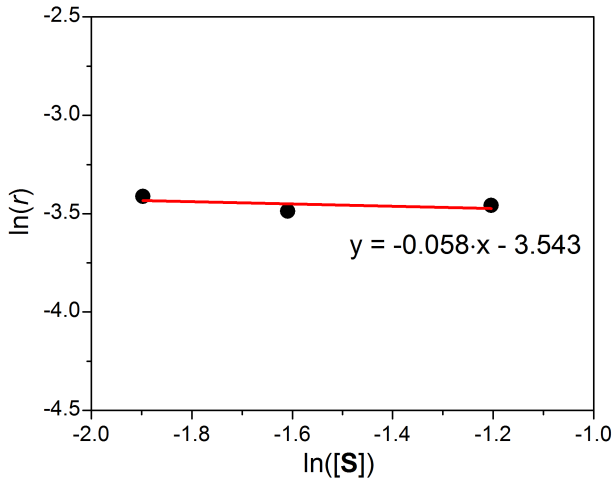

Figure S2. Order plot of the initial hydrogenation rate of **S** (*r*) with respect to the substrate concentration [**S**].

The rate is found nearly independent on the substrate concentration and we determine from the plot $\alpha = -0.058$, very close to a zero-order dependence.

Partial order in [cat]

Table S3. Experimental rates for determination of partial order in [cat]

Entry	[**cat**] ($g_{cat} \cdot L^{-1}$)	r ($mol \cdot L^{-1} \cdot h^{-1}$)
1	2.50	0.0139
2	3.75	0.0225
3	5.00	0.0320
4	6.25	0.0402

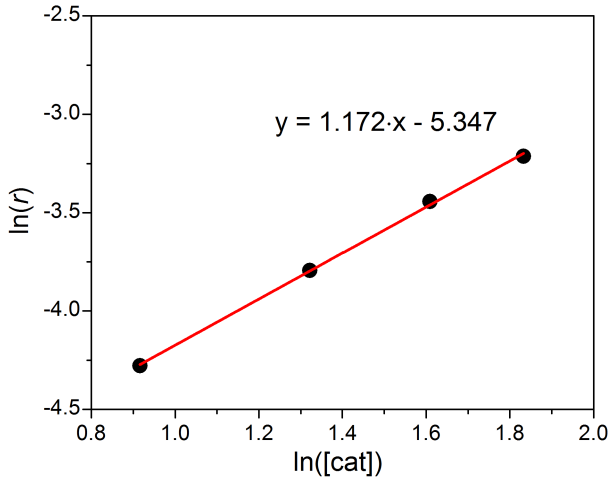

Figure S3. Order plot of the initial hydrogenation rate of **S** (r) with respect to the catalyst concentration [**cat**].

The rate is found to be linearly dependent on the catalyst concentration and we determine from the plot $\beta = 1.172$, very close to a first-order dependence.

Partial order in P_{H_2}

Table S4. Experimental rates for determination of partial orders in P_{H_2}

Entry	P_{H_2} (bar)	r (mol·L^{-1}·h^{-1})
1	5	0.0148
2	10	0.0282
3	15	0.0408
4	20	0.0552

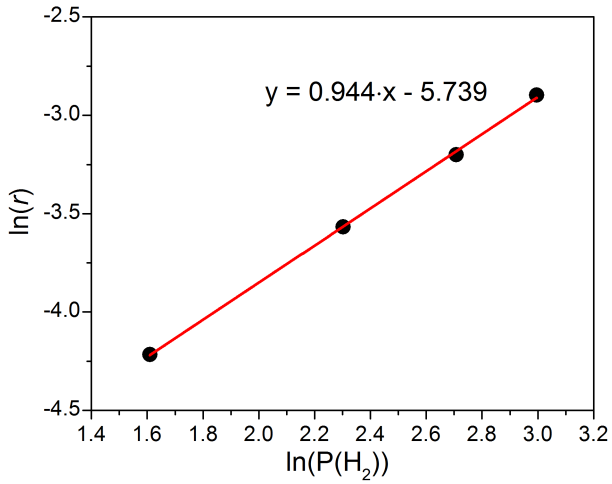

Figure S4. Order plot of the initial hydrogenation rate of **S** (r) with respect to the pressure of H_2 concentration P_{H_2}.

The rate is found to be linearly dependent on the catalyst concentration and we determine from the plot $\gamma = 0.944$, very close to a first-order dependence.

Expressions of adsorption constants

Adsorption constants K_i in the rate equations (**Equations 4** and **5**) can be expressed within a Langmuir-Hinshelwood formalism[2, 3] considering here one type of active Cu sites ($*$) and the equilibria of **S**, $\mathbf{S_{2H}}$, $\mathbf{S_{4H}}$ and a ligand **L** in solution with their respective **S***, $\mathbf{S_{2H}}$*, $\mathbf{S_{4H}}$* and **L*** adsorbates on these sites (**Scheme 1c**). This formalism leads to **Equations S4,** where [$\boldsymbol{i}$] are concentrations in solution, [$\boldsymbol{i}$*] and [$*$] are concentrations of surface species for adsorbates and empty active sites, respectively, and C^0 is the standard concentration (C^0 = 1 $\mathrm{mol \cdot L^{-1}}$). From **Equations S4**, we derive **Equations S5** where we express the fraction θ_i of surface species [$\boldsymbol{i}$*] relative to the total active site concentration $[*]_{tot}$ as a function of the concentrations of species in the liquid-phase [$\boldsymbol{i}$], the adsorption constants K_i and the denominator Γ (**Equation 6**).

Equations S4

(a) $K_A = \dfrac{[\boldsymbol{S}^*]C^0}{[\boldsymbol{S}][*]}$ **(b)** $K_B = \dfrac{[\boldsymbol{S_{2H}}^*]C^0}{[\boldsymbol{S_{2H}}][*]}$ **(c)** $K_C = \dfrac{[\boldsymbol{S_{4H}}^*]C^0}{[\boldsymbol{S_{4H}}][*]}$ **(d)** $K_L = \dfrac{[\boldsymbol{L}^*]C^0}{[\boldsymbol{L}][*]}$

Equations S5

(a) $\theta_{\boldsymbol{A}} = \dfrac{[\boldsymbol{S}^*]}{[*]_{tot}} = \dfrac{K_A[\boldsymbol{S}]}{\Gamma C^0}$ **(b)** $\theta_{\boldsymbol{B}} = \dfrac{[\boldsymbol{S_{2H}}^*]}{[*]_{tot}} = \dfrac{K_B[\boldsymbol{S_{2H}}]}{\Gamma C^0}$ **(c)** $\theta_{\boldsymbol{C}} = \dfrac{[\boldsymbol{S_{4H}}^*]}{[*]_{tot}} = \dfrac{K_C[\boldsymbol{S_{4H}}]}{\Gamma C^0}$

(d) $\theta_* = \dfrac{[*]}{[*]_{tot}} = \dfrac{1}{\Gamma}$ **(e)** $\theta_{\boldsymbol{L}} = \dfrac{[\boldsymbol{L}^*]}{[*]_{tot}} = \dfrac{K_L[\boldsymbol{L}]}{\Gamma C^0}$

Substrate adsorption isotherms

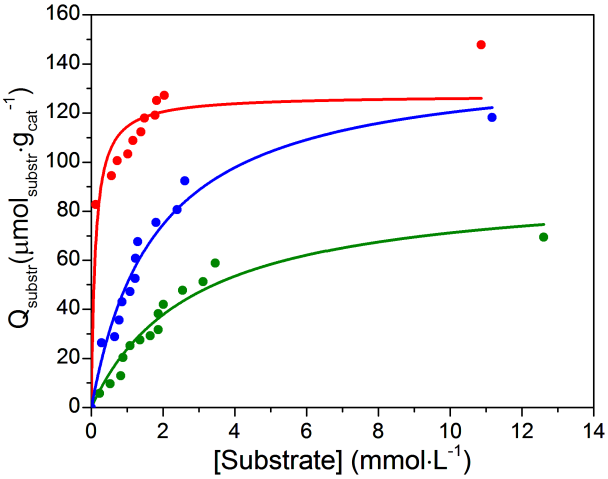

Figure S5. S (red), (*E*)-**S**$_{2H}$ (blue) and **S**$_{4H}$ (green) adsorption isotherms on **Cu/SiO$_2$** at 40 °C (dots) and associated Langmuir associative adsorption isotherms (solid lines).

Substrate chemisorption curves were fitted with a Langmuir associative adsorption isotherm of the formula:

Equations S6

$$Q_i([i]) = Q_i^{max} \cdot \frac{K_i \frac{[i]}{C^0}}{1 + K_i \frac{[i]}{C^0}}$$

where Q_i, Q_i^{max} are respectively coverage at equilibrium and maximal coverage in substrate ***i***, $[i]$ and C^0 respectively concentration and standard concentration (1 mol·L^{-1}) in ***i*** susbtrate and K_i the adsorption equilibrium constant for ***i*** substrate.

Adsorbate geometries and density maps

115

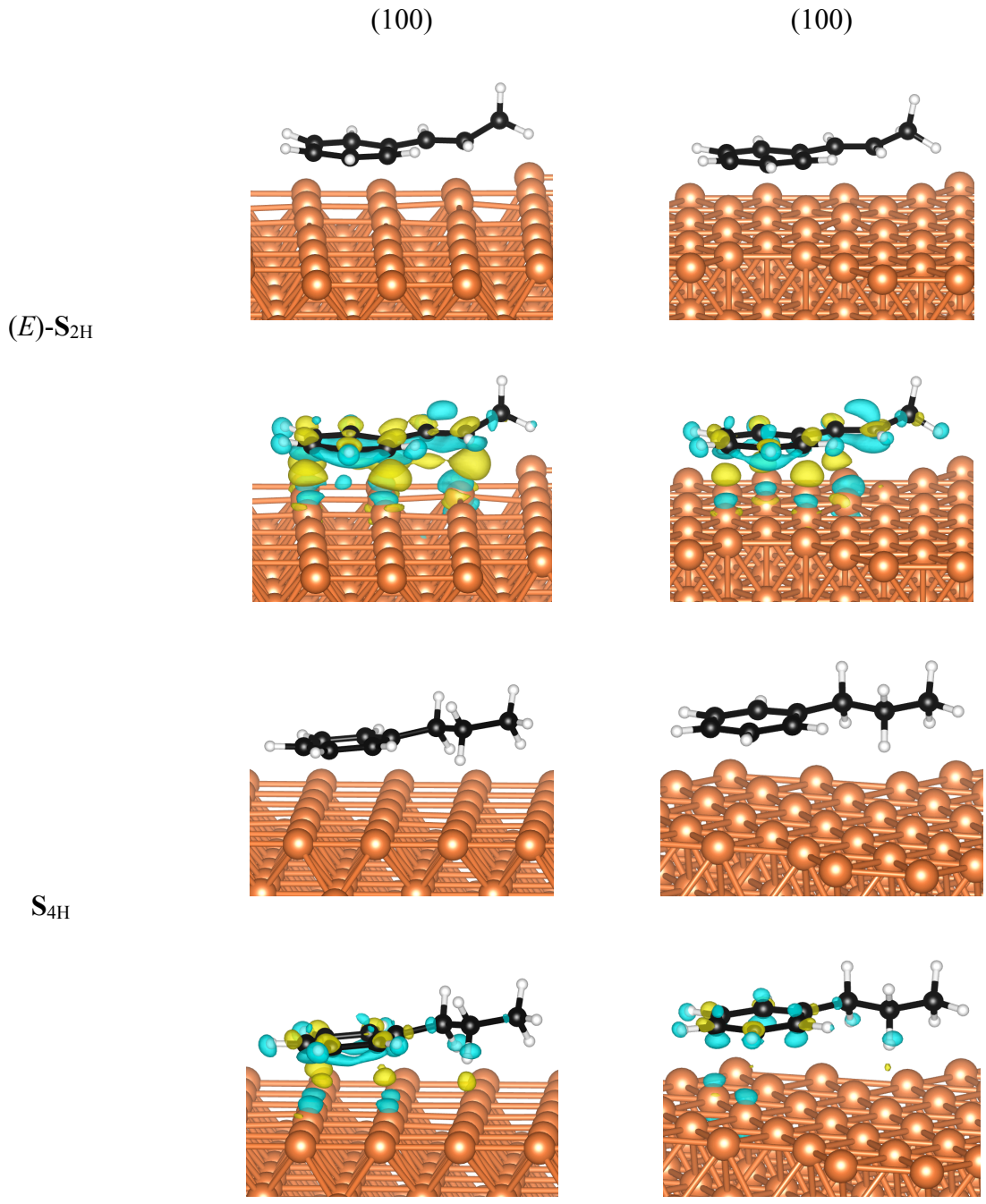

Toluene

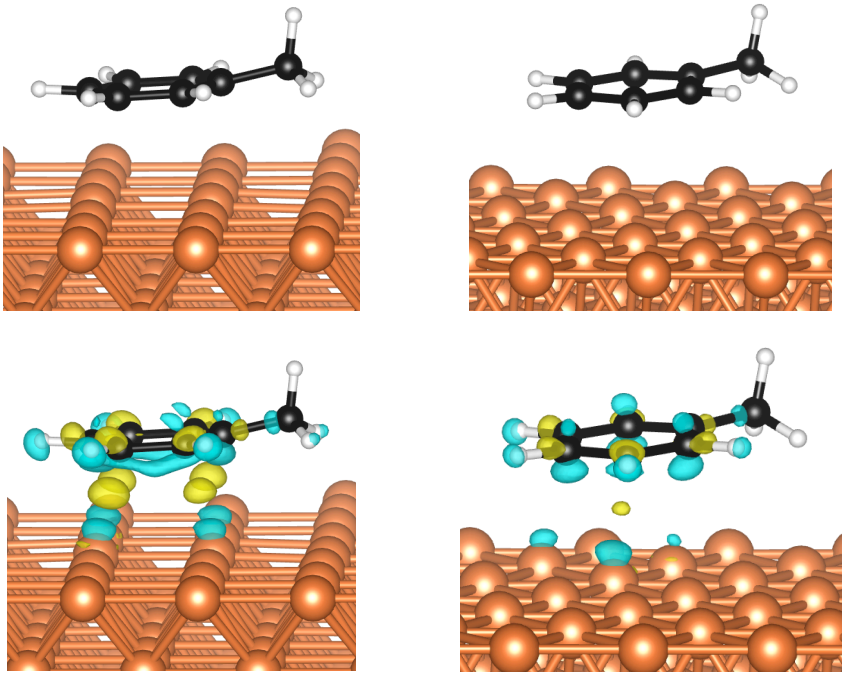

Figure S6. Molecular models for (*E*)-$\mathbf{S}_{2H}$, $\mathbf{S}_{4H}$ and toluene adsorbed on the (100) and (111) terminations of *fcc* copper. The bottom images show the charge density differences (see method section). Yellow and blue colors represent accumulation or depletion of charge density, respectively. The values for isosurfaces are ± 2.5 10^{-3} e·Å^{-3} for all models.

Kinetic data and modelling

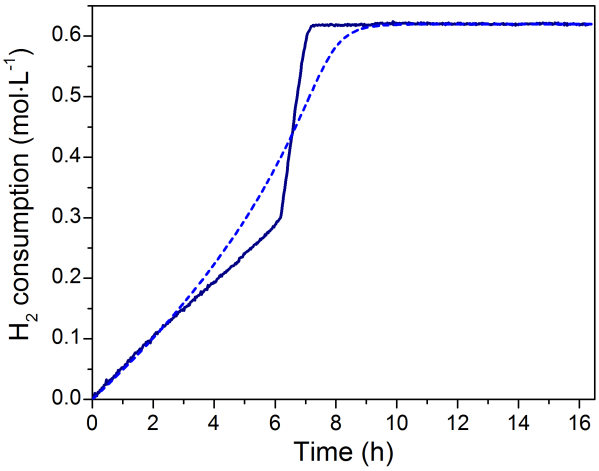

Figure S7. Experimental H_2 consumption profile (solid line) during hydrogenation of **S** at 40 °C on **Cu/SiO$_2$** and the corresponding fit using *K* adsorption constants measured from adsorption isotherms (dashed line).

120

a) **b)**

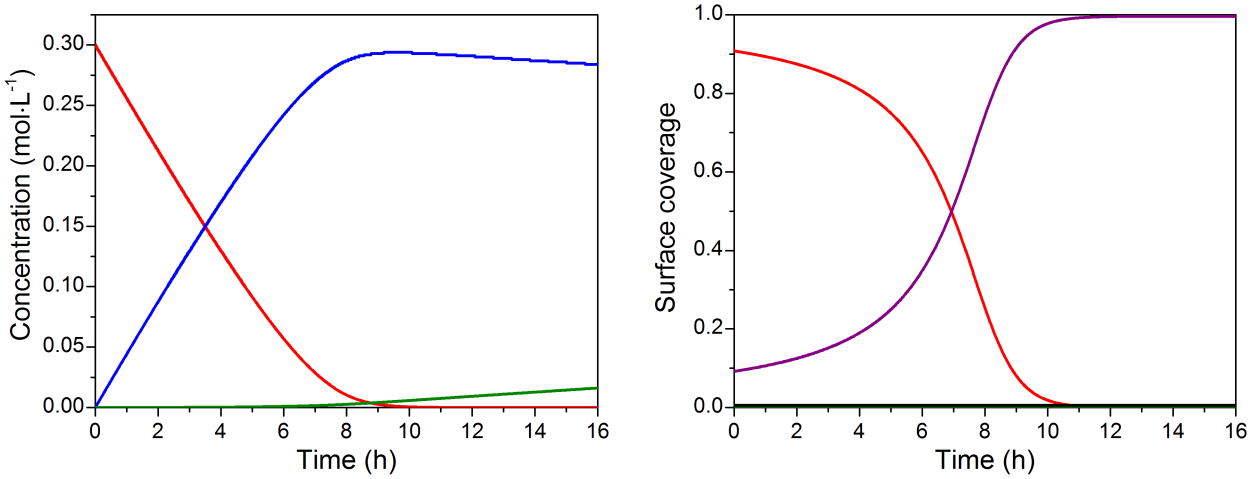

Figure S8. a) Simulated concentrations in **S** (red), **S$_{2H}$** (blue), **S$_{4H}$** (green) and b) surface coverage on **Cu/SiO$_2$** in **S*** (red), **S$_{2H}$*** (blue), **S$_{4H}$*** (green), IMes* (purple) and empty sites * (black) in the presence of IMes in a 1:50 IMes/**S** ratio.

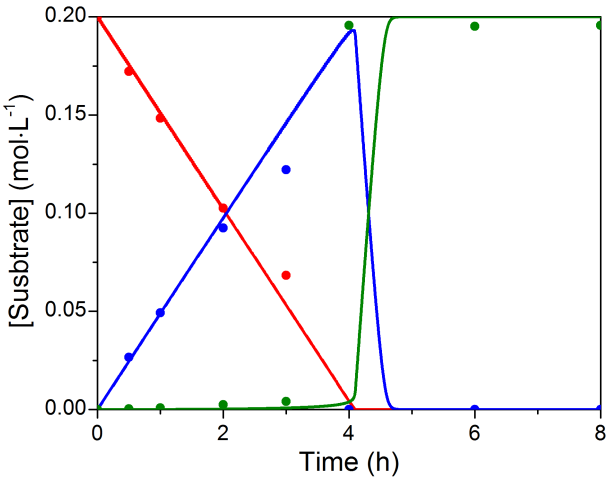

Figure S9. Experimental concentrations **S** (red), $\mathbf{S_{2H}}$ (blue), $\mathbf{S_{4H}}$ (green) from GC analysis (dots) during hydrogenation of **S** at 40 °C, 20 bar H_2 on **Cu/SiO₂** (0.375 mol%; sample and data from ref[4]) and corresponding simulated concentrations using constants from Table 3 (lines).

a)

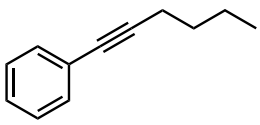

1-phenyl-1-hexyne

b)

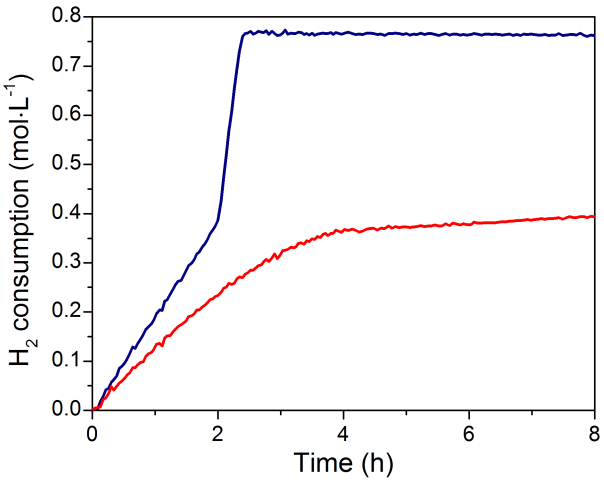

Figure S10. a) Structure of 1-phenyl-1-hexyne and b) H_2 consumption profiles during hydrogenation of 1-phenyl-1-hexyne with **Cu/SiO₂** (ca. 0.8 mol% Cu_{total} and 0.3 mol% $Cu_{surface}$ vs 1-phenyl-1-hexyne) at 10 bar H_2 and 40 °C in the absence (blue) or in the presence (red) of PCy_3 in 1:50 PCy_3/1-phenyl-1-hexyne ratio.

125

References

[1] K. Larmier, S. Tada, A. Comas-Vives, C. Coperet, J. Phys. Chem. Lett., 7 (2016) 3259.
[2] L. Červený, V. Růžička, Cat. Rev., 24 (1982) 503.
[3] L. Červenýa, V. Rûržička, Adv. Catal., 30 (1981) 335.
[4] A. Fedorov, H.J. Liu, H.K. Lo, C. Coperet, J. Am. Chem. Soc., 138 (2016) 16502.